ISSN 0006-2979, Biochemistry (Moscow), 2025, Vol. 90, No. 6, pp. 754-772 © Pleiades Publishing, Ltd., 2025.
Published in Russian in Biokhimiya, 2025, Vol. 90, No. 6, pp. 812-832.

Multiepitope mRNA Vaccine mRNA-mEp21-FL-IDT Provides Efficient Protection against *M. tuberculosis*

Alisa A. Kazakova[1], Galina S. Shepelkova[2], Ivan S. Kukushkin[1], Vladimir V. Yeremeev[2], Roman A. Ivanov[1], and Vasiliy V. Reshetnikov[1,a]*

[1]*Sirius University of Science and Technology, 354340 Sirius Federal Territory, Russia*
[2]*Central Tuberculosis Research Institute, 107564 Moscow, Russia*
[a]*e-mail: reshetnikov.vv@talantiuspeh.ru*

Received January 18, 2025
Revised June 9, 2025
Accepted June 9, 2025

Abstract—Tuberculosis is a leading cause of death from a bacterial infection agent. The development of new tuberculosis vaccines can reduce the number of new cases and tuberculosis-related deaths. One of the most promising areas in vaccination is development of mRNA vaccines, which have already proven their high effectiveness against COVID-19 and other viral infections. Using modern immunoinformatic methods, we developed four new antituberculosis multiepitope mRNA vaccines differing in the encoded adjuvants and codon composition and tested their immunogenicity and protectivity in mice. Most of the developed mRNA vaccines induced the formation of both cellular and humoral immunity. The adaptive response was stronger for the vaccines with the RpfE adjuvant; however, the best protective response was elicited by the mRNA-mEp21-FL-IDT vaccine with the FL adjuvant. This vaccine reduced the mycobacterial load in the lungs of mice infected with *Mycobacterium tuberculosis* and increased their survival rate. Altogether, our results indicate that the mRNA-mEp21-FL-IDT vaccine ensures effective protection against tuberculosis comparable to that provided by the BCG vaccine.

DOI: 10.1134/S0006297925600073

Keywords: mRNA vaccine, tuberculosis, multiepitope vaccines, molecular adjuvants, adaptive immunity, protective immunity

INTRODUCTION

Tuberculosis is an infectious disease caused by the *Mycobacterium tuberculosis* bacterium. In 2023 alone, 10.7 million new cases of tuberculosis have been registered, and 1.25 million people died of this disease [1]. Currently, Bacillus Calmette–Guérin (BCG) is only one certified vaccine against tuberculosis; however, it is ineffective against pulmonary tuberculosis, which is the main form of tuberculosis in adults [2]. In this regard, there is an urgent need for new highly efficient antituberculosis vaccines.

mRNA vaccines have gained widespread recognition due to the success of the RNA-1273 (Moderna) and BNT162b2 (Pfizer) vaccines against SARS-CoV-2. Currently, new mRNA vaccines are being designed against HIV-1, Zika virus, influenza virus, rabies virus, and other pathogens [3-6]. mRNA vaccines present several advantages over other types of vaccines, including low production costs, rapid development, high efficacy, noninfectivity, and the absence of integration into the genome. Although mRNA vaccines have proven their effectiveness and safety [7, 8], researchers have not yet succeeded in creating an antituberculosis mRNA vaccine that would ensure strong protection comparable to that provided by the BCG vaccine [9, 10].

The key role in the effectiveness of mRNA vaccines against bacterial pathogens is played by the target antigen sequences and molecular adjuvants. Currently, the most promising strategy for choosing an antigen for vaccines is the multiepitope design, i.e., inclusion of many individual epitopes from different pathogen's antigens [11, 12]. The design of a multiepitope mRNA vaccine allows the incorporation of the

* To whom correspondence should be addressed.

most immunogenic and safest epitopes [13-16], which will activate cytotoxic T lymphocytes (CTL), helper T lymphocytes (HTL), and B cells when presented by the major histocompatibility complex (MHC). As a rule, the antigenic proteins used in the vaccine creation are surface and secreted proteins of a pathogen, which are the first to come into contact with host's immune system.

The immunogenicity and safety of epitopes are determined by their affinity to the MHC, stability (resistance to proteolytic cleavage in a cell), and lack of homology with the organism's own proteins. The three-dimensional structure is especially important for the B cell epitopes, since B cell receptors recognize conformational epitopes on the antigen surface. The binding to the epitope leads to the activation of B cells and their differentiation into plasma cells that produce the antibodies specific to this epitope.

T cell epitopes (CTL and HTL) are formed by the antigen cleavage in the proteasome and binding to the MHC class I (for $CD8^+$ T cells) or class II (for $CD4^+$ T cells). The MHC–epitope complex is transported to the cell surface, where it is recognized by T cells through the T cell receptors, leading to the activation of T cells and triggering of the immune response.

Beside the epitopes, the effectiveness of mRNA vaccines is determined to a great extent by the encoded molecular adjuvants. For example, incorporation of the FMS-like tyrosine kinase-3 ligand (FL) as an encoded adjuvant increased the level of Th1 cytokine (IFN-γ and IL-12) production, the number of T cells secreting IFN-γ, the activity of cytotoxic T lymphocytes, and the level of IgG antibodies, which together allowed to develop an antituberculosis DNA vaccine with a better efficacy than BCG [17]. Other molecules have also been used as adjuvants in antituberculosis vaccines, including resuscitation-promoting factor E (RpfE), which helps restore the viability of *M. tuberculosis* and ensures the activation of dendritic cells (DCs), as well as heparin-binding hemagglutinin (HBHA) and 50S ribosomal protein (Rv0652), which act as bacterial agonists of Toll-like receptors (TLRs) and promote the activation of TLR4. RpfE, HBHA, and Rv0652 induce the maturation of DCs by enhancing the surface expression of maturation markers (CD40, CD80/CD86, and class I/II MHC) and production of IL-6, IL-1β, IL-23p19, IL-12p70, and TNF-α in a TLR4-dependent manner [18-20]. RpfE also promotes the differentiation of $CD4^+$ T cells into Th1 and Th17 subpopulations through the modulation of DC function.

Beside the coding sequence of antigens, molecular adjuvants, and signal peptides [21, 22], the secondary structure of the RNA molecule itself plays an important role in the effectiveness of mRNA therapeutics, as it determines the translational efficiency of mRNA and its stability in the cells [23, 24].

In our study, we focused on designing an effective multiepitope mRNA antituberculosis vaccine by *in silico* immunoinformatic methods, which substantially reduced the duration and cost of vaccine development due to the rapid and effective prediction of suitable vaccine antigens, epitopes, and adjuvants [25]. We employed two sequences of molecular adjuvants – RpfE and FL – and used two contrasting strategies for the RNA secondary structure optimization. To test the functional efficacy of the four newly developed mRNA vaccines and to compare them to BCG, we evaluated their immunogenicity and protectivity *in vivo* in mice with the opposite sensitivity to tuberculosis.

MATERIALS AND METHODS

The choice of target proteins. All amino acid sequences were obtained from the NCBI Protein (https://www.ncbi.nlm.nih.gov/) and UniProt (http://www.Uniprot.org) databases. Linear B lymphocyte (LBL), CTL, and HTL epitopes with the optimal characteristics were chosen within the amino acid sequences of selected *M. tuberculosis* proteins.

Prediction and evaluation of LBL, CTL, and HTL epitopes. To predict the LBL epitopes, we selected 10 *M. tuberculosis* antigens that induce a pronounced IgG response and/or are membrane proteins [26, 27]: ESAT6, CFP10, Ag85A, Ag85B, PE, PPE55, PPE68, MPT83, HRP1, and HspX. The LBL epitopes were selected with the ABCpred online server (https://webs.iiitd.edu.in/raghava/abcpred/ABC_submission.html) [28], which predicts epitopes using a recurrent neural network trained on epitopes from the Bcipep database (https://webs.iiitd.edu.in/raghava/bcipep/info.html) [29]. The parameters applied for the epitope search were as follows: LBL epitope length, 16 amino acid (a.a.) residues; specificity threshold, 0.51; overlapping filter: ON. All LBL epitopes predicted by the server were subjected to subsequent analysis.

The CTL epitopes were chosen using the Next Generation T Cell Prediction Class I online resource (https://nextgen-tools.iedb.org/) [30]. The epitope lengths were set to 9-10 a.a. The full reference set of human leukocyte antigens (HLA) and the NetMHCpan 4.1 EL mathematical model were used to predict the epitopes. The obtained CTL epitopes were sorted by IC50, and peptides with IC50 < 500 were selected for subsequent analysis.

The HTL epitopes were predicted with the MHC-II Binding Predictions server (http://tools.iedb.org/mhcii/). The length of the epitopes was set to 15 a.a. The epitopes were predicted using the full reference set of HLA and the NetMHCIIpan 4.1 EL mathematical model. The obtained peptides were sorted by their

percentile rank, and epitopes with a rank >90 were selected for further analysis.

To predict the potential autoimmunogenicity, all selected epitopes were checked for homology with the human and mouse proteomes using the protein–protein BLAST service (https://blast.ncbi.nlm.nih.gov/Blast.cgi?PROGRAM=blastp&PAGE_TYPE=BlastSearch&LINK_LOC=blasthome) and *Homo sapiens* and *Mus musculus* protein databases (Taxid:9606 and Taxid:10090, respectively). To prevent the autoimmune response, all chosen peptides lacked homologs among human and mouse proteins with an E-value < 0.1 [31].

To predict the antigenicity, the selected epitopes were analyzed with the VaxiJen software v3.0 (https://www.ddg-pharmfac.net/vaxijen3/) [32]. The epitopes that were identified as potentially antigenic with a probability of at least 66% according to the analysis results were subjected to further investigation. To predict the allergenicity of the epitopes, the AllerTOP server v2.0 (https://www.ddg-pharmfac.net/AllerTOP/) was used with the default parameters; only nonallergenic epitopes were selected [33]. To predict the toxicity of the epitopes, we used the next-generation ToxiPred2 web server (https://webs.iiitd.edu.in/raghava/toxinpred2/ige.html) under the MERCI prediction model [34]. Only the epitopes that were found to be antigenic, nonallergenic, and nontoxic were selected for further analysis.

Next, the LBL epitopes were assessed for their putative ability to induce in a complex with MHC the synthesis of IgG and IgE using the IgPred Web server (https://webs.iiitd.edu.in/raghava/igpred/prot-varipred.html) with a threshold of 0.9 [35].

The HTL epitopes were tested for their tentative ability to induce in a complex with MHC the synthesis of IFN-γ, IL-4, and IL-10. To evaluate the secretion of IFN-γ, we employed the IFNepitope Web service (https://webs.iiitd.edu.in/raghava/ifnepitope/predict.php) using the hybrid prediction approach "SVM + motif" with the "IFN-γ versus non IFN-γ" prediction module [36]. The secretion of IL-4 was assessed with IL4pred (https://webs.iiitd.edu.in/raghava/il4pred/predict.php) [37] using the "SVM + motif" hybrid prediction model with a threshold of 0.2. To predict the secretion of IL-10, IL-10Pred (https://webs.iiitd.edu.in/raghava/il10pred/predict3.php) was utilized with the SVM predictive model with a threshold of −0.3 [38]. Only the epitopes that induced the secretion of IFN-γ but not of IL-4 or IL-10 were selected for further studies.

The final vaccine sequence included 7 LBL epitopes, 7 HTL epitopes, and 7 CTL epitopes.

Analysis of MHC allele frequency in the population. The estimated coverage of the population was predicted for all the epitopes selected at the previous stages using the corresponding MHC I and MHC II alleles with the Population Coverage tool (http://tools.iedb.org/population/) in the IEDB 59 database [39]. The prediction was made using the full set of MHC alleles similar to the set utilized at the epitope prediction stage, as well as the full "Russia" dataset. Based on the analysis of population coverage, we selected epitopes with >90% prevalence of respective MHC alleles in the population.

Molecular docking between T-lymphocyte epitopes and MHC alleles. Molecular docking of the HTL and CTL epitopes was performed on the CABS-dock Web server (https://biocomp.chem.uw.edu.pl/CABSdock/) [40]. After the docking, we used the HawkDock server (http://cadd.zju.edu.cn/hawkdock/) to estimate the binding free energy in order to find the best conformation identified by CABS-dock [41].

The selected MHC I alleles were HLA-A*11:01 (PDB ID: 6ID4), HLA-A*02:01 (PDB ID: 7RTD), and HLA-A*24:02 (PDB ID: 5WWI); the selected MHC II alleles were HLA-DRB1*01:01 (PDB ID: 1AQD), HLA-DRB1*15:01 (PDB ID: 8TBP), HLA-DRB1*07:01 (PDB ID: 7Z0Q), and HLA-DPA1*01:03/HLA-DPB1*02:01 (PDB ID: 3LQZ). These alleles were chosen as some of the most common alleles in the Russian population (https://allelefrequencies.net/default.asp) [42].

The resulting docking models were assessed using the root-mean-square distance (RMSD), a parameter indicating the quality of docking and directly related to the quality of ligand–receptor binding. According to the developers' assessment, the docking poses with RMSD > 3.00 Å have only few key interactions characteristic of true docking positions, while RMSD < 3 Å indicates a large number of key interactions, suggesting strong ligand binding. RMSD from 3 to 5.5 Å corresponds to a moderate strength of ligand binding, and at RMSD > 5.5 Å, the ligand presumably does not bind at all.

Design of multiepitope vaccine proteins and vaccine mRNAs. We used four types of cleavable linkers (EAAAK, GPGPG, KK, and AAY) in the design of the vaccine protein to ensure the hydrolysis and necessary flexibility/rigidity of the synthesized protein molecules for the efficient epitope presentation. The EAAAK linker was placed between the tissue plasminogen activator (tPA) and the adjuvant sequences to improve the stability of the fusion protein [43]. The GPGPG and AAY linkers were placed between the HTL and CTL epitopes, respectively, to improve the presentation [44]. The HTL epitopes were connected to each other via the GPGPG linkers, the LBL epitopes – via the KK linkers, and the CTL epitopes – via the AAY linkers. The optimized Kozak sequence (GCCACAAUGgg) was included in the mRNA sequence [45]. A special stop codon sequence (UGAUGAUGA) was chosen to achieve the maximal translation termination. Two signal sequences were added to the mRNA to strengthen the antigen presentation:

the tPA secretory signal (UniProt ID: P00750) was placed at the 5′ end, and the MHC I-targeting domain (MITD; UniProt ID: Q8WV92) was placed at the 3′ end.

The full-length RpfE (CCP45243.1) and FL (NP_001450.2) were used as encoded adjuvants. RpfE (Rv2450c) was chosen because it binds to TLR4, induces proliferation of T cells and differentiation into Th1 and Th17 lymphocytes with a pronounced antimycobacterial activity, stimulates the production of proinflammatory cytokines, promotes the cellular immune response, and enhances the adaptive immune response [18]. FL, which is a growth factor, stimulates the growth of T cells, B cells, and DCs, increases the immunogenicity of DNA vaccines; and enhances the recruitment and expansion of DCs, thereby contributing to the formation of effective immune response [17].

The TPL sequence was used as the 5′ untranslated region (UTR). The TPL has a high median ribosome loading and improves the mRNA translational efficiency (https://optimus5.cs.washington.edu/MRL) [46, 47]. The 3′ UTR sequence from the RNA-1273 vaccine against SARS-CoV-2 (Moderna) served as the 3′ UTR. Furthermore, to increase the mRNA stability, a standard 110-nt polyA tail and the AG sequence were added downstream of the T7 promoter in the expression cassette. The AG sequence ensures the cotranscriptional incorporation of the synthetic cap analog $m_2^{7,3'}$-OGpppAmG (CapAG) during transcription *in vitro*.

Therefore, the overall structure of the vaccine mRNA was as follows: 5′-cap → 5′ UTR → Kozak sequence → tPA signal peptide → EAAAK linker → RpfE/FL (adjuvant) → GPGPG linker → HTL epitopes → KK linker → LBL epitopes → AAY linker → CTL epitopes → AAY linker → MITD → stop codons → 3′ UTR → polyA tail (Fig. 1). Four mRNA sequences were generated: mRNA-mEp21-RpfE-LD, mRNA-mEp21-FL-LD, mRNA-mEp21-RpfE-IDT, and mRNA-mEp21-FL-IDT that differed in the adjuvant sequence (RpfE or FL) and optimization of the mRNA secondary structure (LD or IDT).

Prediction of antigenicity, allergenicity, toxicity, and physicochemical properties of vaccine proteins. For the analysis of antigenicity, allergenicity, and toxicity of vaccine proteins, we used the amino acid sequences that included the adjuvants, epitopes, and linkers, but lacked the tPA and MITD sequences. The antigenicity of the potential vaccines was predicted with the VaxiJen server v3.0. We also used the ANTIGENpro server (https://scratch.proteomics.ics.uci.edu/) based on the microarray data and machine learning algorithms [48]. The allergenicity, toxicity, and homology of the vaccine proteins were assessed with the AllerTOP v.2.0, ToxiPred2, and BLAST, respectively, as described above.

The physicochemical parameters of protein sequences lacking the tPA and MITD fragments were evaluated with the Expasy server (https://web.expasy.org/protparam/) [49]. The examined characteristics included the number of amino acid residues, molecular weight, theoretical isoelectric point (pI), aliphatic index (AI), instability index (II), and global average hydropathicity (GRAVY).

Determination and confirmation of the tertiary structure of the vaccine proteins. The hypothetical tertiary structures were obtained using Robetta (https://robetta.bakerlab.org/submit.php) [50] and then evaluated with the ERRAT, Verify 3D, and PROCHECK web services (https://saves.mbi.ucla.edu/).

Prediction of conformational B-cell epitopes. The tertiary structure of a protein can give rise to new conformational B cell epitopes [51]. To predict both linear and conformational B cell epitopes, we used the ElliPro tool (http://tools.iedb.org/ellipro/), which analyzes geometric characteristics of 3D models and offers the best area under the curve (AUC) (0.732) for any protein model [52, 53].

Molecular docking of vaccine proteins with TLR4. The docking was performed between each putative vaccine protein and TLR4 (PDB ID: 3FXI) using the ClusPro 2.0 server (https://cluspro.bu.edu/home.php) and the PIPER algorithm [54]. RpfE (TLR4 agonist) served as a positive control [18]. The binding free energy (ΔG) and the dissociation constant (K_d) were calculated at 37°C with the help of the PRODIGY tool from the HADDOCK server (https://rascar.science.uu.nl/prodigy/) [55]. The PDBsum web server (https://www.ebi.ac.uk/thornton-srv/databases/pdbsum/Generate.html) was used to analyze and visualize the receptor–ligand interactions [56].

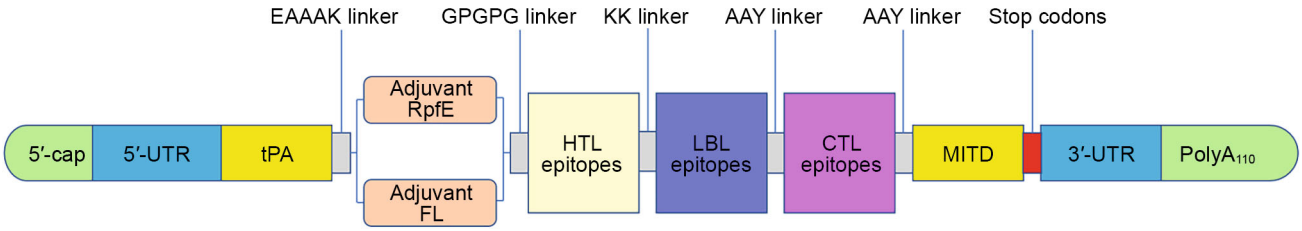

Fig. 1. Structure of developed mRNA vaccines. Four mRNA sequences were generated: mRNA-mEp21-RpfE-LD, mRNA-mEp21-FL-LD, mRNA-mEp21-RpfE-IDT and mRNA-mEp21-FL-IDT, differing in the adjuvant sequence (RpfE or FL) and optimization of the mRNA secondary structure (LD or IDT). 7 HTL epitopes, 7 LBL epitopes, and 7 CTL epitopes were included in each vaccine variant.

***In silico* immunization.** The time course of the immune response was simulated for each vaccine with the C-ImmSim server (https://kraken.iac.rm.cnr.it/C-IMMSIM/index.php?page=1) employed [57]. Three *in silico* immunizations (injections) of 1000 units of vaccine per dose were performed on days 1, 28, and 56 of the simulation. The remaining parameters were defaults.

Optimization of codon composition and removal of miRNA-binding sites. Optimization algorithms are commonly used to increase the mRNA stability and translation efficiency. Optimization was performed with the following algorithms: Linear Design (https://github.com/LinearDesignSoftware/LinearDesign), RiboTree (https://github.com/philarevalo/RiboTree), IDT (https://eu.idtdna.com/pages), genewiz (https://www.genewiz.com/en-GB/), and iCodon (https://bazzinilab.shinyapps.io/icodon/) [24, 58, 59]. The obtained mRNA sequences were analyzed in the Superfolder (https://github.com/eternagame/superfolder-covid-mrna-vaccines).

The Superfolder, which includes special software packages for determining the degradation time, secondary structure, Δ*G*, and other critical characteristics of mRNA, was used to evaluate the following parameters: mRNA half-life, average unpaired probability (AUP; the total proportion of unpaired nucleotides; lower AUP increases the life span of mRNA), AUP init 14 (the total proportion of unpaired nucleotides within the first 14 nucleotides; higher AUP init 14 increases the translatability of mRNA), and codon adaptation index (CAI, codon optimization parameter; higher CAI increases the translatability of mRNA). The *in silico* parameters predicted by the Superfolder programs have not been experimentally verified.

For further work, we chose the Linear Design and IDT algorithms because according to the *in silico* modeling results, Linear Design increased the half-life of RNA better than the other algorithms, whereas IDT helped to achieve the optimal mRNA translatability.

To prevent the cleavage and translation inhibition of mRNA, we searched the designed mRNA sequences for the binding sites for *H. sapiens* and *M. musculus* miRNAs using the miRDB website (https://mirdb.org/custom.html). If the probability of the binding site presence was ≥65 (conventional units of this server; scale, from 0 to 100), the corresponding codons were replaced with synonymous ones to decrease the probability below 65, after which the resulting sequences were rechecked for the presence of miRNA-binding sites and translated *in silico* to correct possible errors caused by the codon replacement (http://molbiol.ru/scripts/01_13.html).

Animal experiment design. Female mice of the C57BL/6JCit (B6) (genetically resistant to tuberculosis) and I/StSnEgYCit (I/St) (genetically sensitive to tuberculosis [60]) strains aged 3 to 4 months and weighing at least 21 g were used in the experiments. The animals were kept under standard conditions with the *ad libitum* access to food and water at the Animal Facility of the Tuberculosis Research Institute (Moscow, Russia).

To assess the immunogenicity of the candidate vaccines, B6 mice were divided into 7 groups (5 mice per group). The animals of the experimental groups were immunized intramuscularly twice (5 μg/mouse) at an interval of 4 weeks with one of the four mRNA vaccines (mRNA-mEp21-RpfE-IDT, mRNA-mEp21-FL-IDT, mRNA-mEp21-RpfE-LD, or mRNA-mEp21-FL-LD). Mice receiving lipid nanoparticles (LNPs) without mRNA or phosphate-buffered saline (PBS (Sigma-Aldrich, USA), pH 7.5) served as negative controls. Positive controls were mice that were inoculated subcutaneously with 100,000 colony-forming units (CFU) of BCG one time, five weeks before the experiment.

Four weeks after the second immunization, the antigen-specific production of IFN-γ was assessed by the ELISpot assay *ex vivo* in isolated splenocytes. The titer of IgGs (the maximum serum dilution at which specific IgGs are detected) to the *Mycobacterium tuberculosis* sonicate, which was obtained by ultrasonically disintegrating bacterial cells, was determined in animal blood serum. The serum was diluted with PBS at a 1 : 50 to 1 : 400 ratio. The intensity of the humoral response was assessed by absorption at 450 nm according to the previously described method [61].

The protective properties of mRNA vaccines were evaluated in I/St mice genetically sensitive to tuberculosis. The animals were divided into seven groups each containing 15 mice. Mice from 4 groups were injected with the mRNA-mEp21-RpfE-IDT, mRNA-mEp21-FL-IDT, mRNA-mEp21-RpfE-LD or mRNA-mEp21-FL-LD vaccines; one group was immunized with the BCG, and two groups served as negative controls (mice injected with mRNA-free LNPs and PBS (pH 7.5)). Immunization with the mRNA vaccines was performed twice with an interval of 4 weeks intramuscularly at a dose of 5 μg/mouse. Four weeks after the second immunization, the mice were infected intravenously with the virulent *M. tuberculosis* H37Rv strain at a dose of 500,000 CFU/mouse. The BCG vaccination was performed once subcutaneously at a dose of 100,000 CFU/mouse 5 weeks before the infection. The weight loss in the infected mice was assessed by weekly weighing the animals. Fifty days after the infection, the mycobacterial load of the spleen and lungs (CFU) (5 mice/group) and the dynamics of mouse death (10 mice/group) were evaluated.

Cloning and *in vitro* transcription. The constructs for subsequent *in vitro* RNA transcription were cloned into the commercial pSmart vector (Lucigen, USA) with the introduced polyA tail.

The 5′ and 3′ UTRs were fused to the coding sequence by the overlap PCR. The resulting insert consisting of the 5′ UTR, coding sequence, and 3′ UTR was cloned into the vector at the *Eco*RI and *Bgl*II restriction sites. The obtained vectors were used for the transformation of NEB-stable cells (New England Biolabs, UK) grown at 30°C on a shaker (180 rpm). The nucleotide sequence of the construct was confirmed by Sanger sequencing. Plasmid DNA was isolated with a Qiagen Plasmid Maxi Kit (Qiagen, USA) and linearized at the unique *Ahl*I restriction site located after the polyA tail.

In vitro transcription was performed in the reaction mixture containing 5 μg of the linearized plasmid, reagents from the RNA-20 Kit (Biolabmix, Russia), 1.2 mM synthetic analog $m_2^{7,3'}$-OGpppAmG (CapAG; Biolabmix), 40 U of RiboCare ribonuclease inhibitor (Evrogen, Russia), and 0.002 U of inorganic pyrophosphatase (New England Biolabs) according to the manufacturer's protocol. A standard set of nucleotides (ATP, GTP, CTP, UTP) was used for *in vitro* transcription. The reaction was carried out for 2 h at 37°C, after which 3 mM each ribonucleoside triphosphate was added, and the reaction mixture was incubated for another 2 h. DNA was hydrolyzed with RQ1 nuclease (Promega, USA), and RNA was precipitated with LiCl (final concentration, 0.32 M) and EDTA (final concentration, 20 mM; pH 8.0), followed by incubation on ice for 1 h. The length and purity of the synthesized RNA molecules were assessed by capillary electrophoresis in a Qsep100 Bio-Fragment Analyzer (BiOptic, Taiwan).

mRNA encapsulation into LNPs. RNA was dissolved at 0.2 mg/ml in 10 mM citrate buffer (pH 3.0) and mixed with lipids dissolved in absolute ethanol in a microfluidic cartridge in a NanoAssemblr™ nanoparticle formulation system (Precision Nanosystems, Canada). The lipid mixture contained 42.7% cholesterol (Sigma-Aldrich), 23.15% synthetic lipid ALC-0315 (BroadPharm, USA), 9.4% 1,2-distearoyl-sn-glycero-3-phosphocholine (DSPC; Avanti Polar Lipids, USA); 1.6% polyethylene glycol 2000 (PEG 2000; BroadPharm); and 23.15% cationic lipid SM-102 (Cayman Chemical, USA). The content of mRNA in the LNPs was 0.04% (by weight). To obtain the LNPs, the aqueous and alcohol phases were mixed at a 3 : 1 (*v*/*v*) ratio; the total mixing rate was 10 ml/min. The obtained particles were dialyzed against PBS (pH 7.4) for 18 h. The quality of the LNPs was assessed using four parameters: particle size, polydispersity index (Zetasizer Nano ZSP, USA), mRNA loading, and RNA integrity. Particle measurements were performed with a Nanobrook Series instrument (Brookhaven Instruments, USA) in a DTS0012 cuvette. The original LNP suspension was diluted 100-fold with PBS (pH 7.4). The concentration of mRNA packed into the LNPs was calculated from the difference in fluorescence before and after disruption of the nanoparticles stained with RiboGreen (Thermo Fischer Scientific, USA). The particles were disrupted with Triton X-100 (Sigma-Aldrich). The fraction of RNA encapsulated into the LNPs in all samples was more than 90% of total (encapsulated + free) RNA. The particle size was 97-118 nm, and the polydispersity index was 0.149-0.186. The RNA quality and integrity in the particles was assessed by capillary electrophoresis with a Qsep100 Bio-Fragment device after LNPs disruption (Online Resource 1).

Quantitative assessment of the T cell response to immunization. The number of splenocytes secreting IFN-γ in response to the stimulation with the *M. tuberculosis* sonicate (soluble fraction of the ultrasonic lysate of *M. tuberculosis* H37RV cells) was determined by the ELISpot assay using a Mouse IFN-γ ELISpot Kit (BD, USA) and an AEC substrate kit (BD), which allowed to quantify the level of the T cell response in immunized mice.

Splenocytes were isolated from the spleen of immunized and control mice under sterile conditions as described previously [62]. The splenocytes were seeded at 200,000 cells/well in ELISpot multi-well plates containing a PVDF membrane (BD) and simultaneously stimulated by adding the *M. tuberculosis* sonicate (10 μg/ml). The total volume of the liquid in each well was brought up to 200 μl with RPMI 1640 culture medium (PanEco, Russia) supplemented with 10% fetal bovine serum (Biowest, France) and the cells were incubated for 20 h in a CO_2 incubator (5% CO_2, 37°C). The cells that had not been stimulated and cells stimulated with concanavalin A (Sigma-Aldrich) at a dose of 5 μg/ml served as the negative and positive controls, respectively. Spots corresponding to splenocytes secreting IFN-γ were counted with an S6 Ultra ELISpot Reader (ImmunoSpot, USA).

Mycobacterial antigens. Mycobacterial antigens were kindly provided by V. G. Avdienko. *M. tuberculosis* cells (strain H37Rv) disrupted by sonication were used as antigens. To obtain the sonicate, mycobacteria were grown in Sotona synthetic broth (HiMedia, India) for 28 days at 37°C. The washed bacterial mass was disintegrated by sonication with a Soniprep 150 Ultrasonic Disintegrator (MSE, United Kingdom) according to the procedure described in [63]. Protein concentration was determined by the Bradford method.

Determination of the titers of IgG against *M. tuberculosis* antigens. The titers of IgG against mycobacterial antigens were determined in mouse blood serum by the enzyme immunoassay using the previously described technique [61]. Briefly, 96-well plates (Helicon, Russia) were coated with the mycobacterium sonicate (10 μg/ml in 50 mM carbonate-bicarbonate buffer, pH 6.1) and incubated for 18-hour at 4°C. Next, mouse blood serum from the immunized and control animals was added to the wells at the dilutions from 1 : 50 to 1 : 400. The reaction was visualized with

horseradish peroxidase-labeled polyclonal antibodies against mouse IgG (Jackson ImmunoResearch Laboratories, USA) using tetramethylbenzidine (TMB; R&D Systems, USA) as a peroxidase substrate.

Evaluation of the protective response after immunization with the mRNA vaccine. The mycobacterial load in the internal organs of infected mice was analyzed on the 50th day after the infection. Spleen and lung tissue homogenates were prepared under sterile conditions. Serial 10-fold dilutions of the homogenates were plated onto Petri dishes (50 µl per dish) with Middlebrook agar 7H10 (Liofilchem, Italy) and incubated at 37°C. After 21 days, the macrocolonies of *M. tuberculosis* H37Rv were counted in the dishes, and these data were converted to the colony number per organ.

Statistical analysis. The data were processed by the one-way ANOVA with the Dunnett's correction for multiple comparisons. The overall survival was estimated by the Kaplan–Meier method. The significance of differences in the overall survival was calculated by the Mantel–Cox log-rank test. The differences between the groups were considered statistically significant at $p < 0.05$. Data analysis and visualization were performed with the GraphPad Prism 9.5.1 software.

RESULTS

Formation of adaptive immunity and effective protection against *M. tuberculosis* via activation of B and T lymphocytes can achieved by selection of optimal HTL, CTL, and LBL epitopes for the antituberculosis vaccine. In this work, we used various immunoinformatic tools to predict and evaluate B- and T-cell epitopes. The efficacy and safety of all obtained epitopes were assessed by analyzing their coverage in the population of the Russian Federation, antigenicity, nonallergenicity, nontoxicity, and autoimmunogenicity (Fig. 2). In total, seven epitopes of each type were chosen for the prospective antituberculosis vaccine. Also, the tPA and MITD sequences were inserted into the coding sequence to direct the encoded protein to the endoplasmic reticulum and Golgi apparatus for its secretion and presentation by the MHC molecules. Furthermore, it is known that the tPA sequence increases the immunogenicity of a vaccine without changing the balance between the Th1 and Th2 immune responses [64, 65]. We assumes that the inclusion of two signal sequences would ensure a balance between the secretion of the target peptide and its

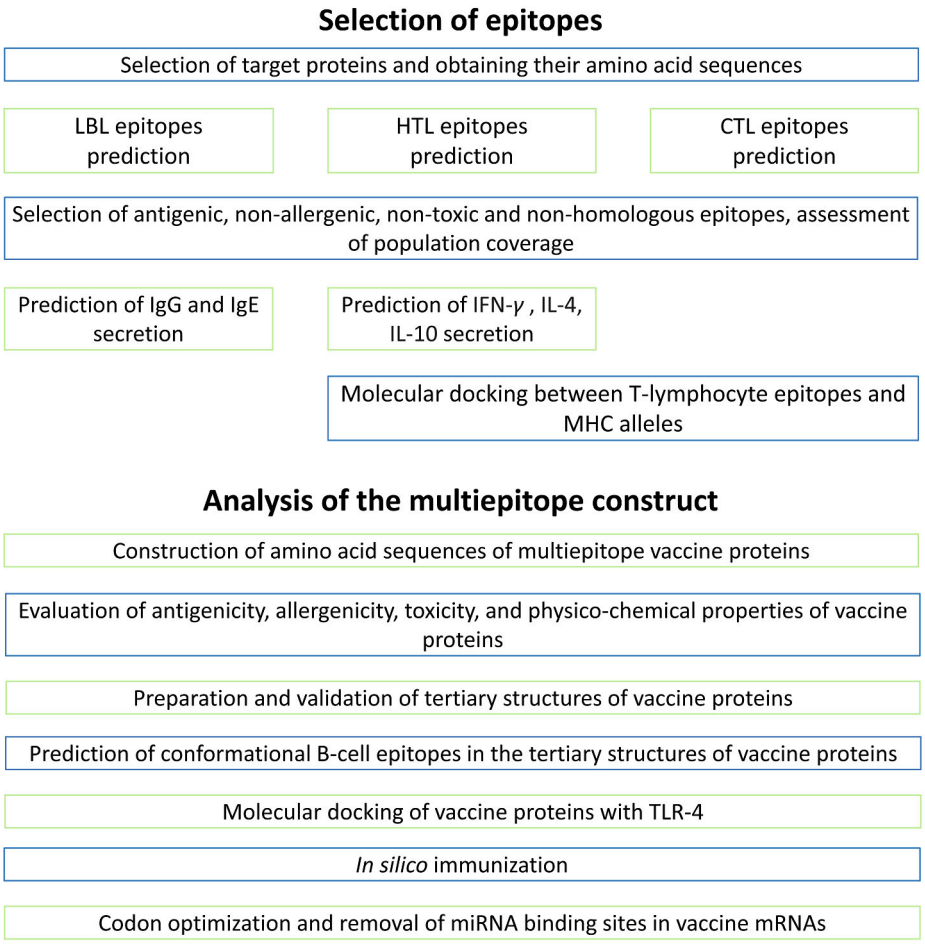

Fig. 2. Stages in the development of the multiepitope mRNA vaccine against tuberculosis.

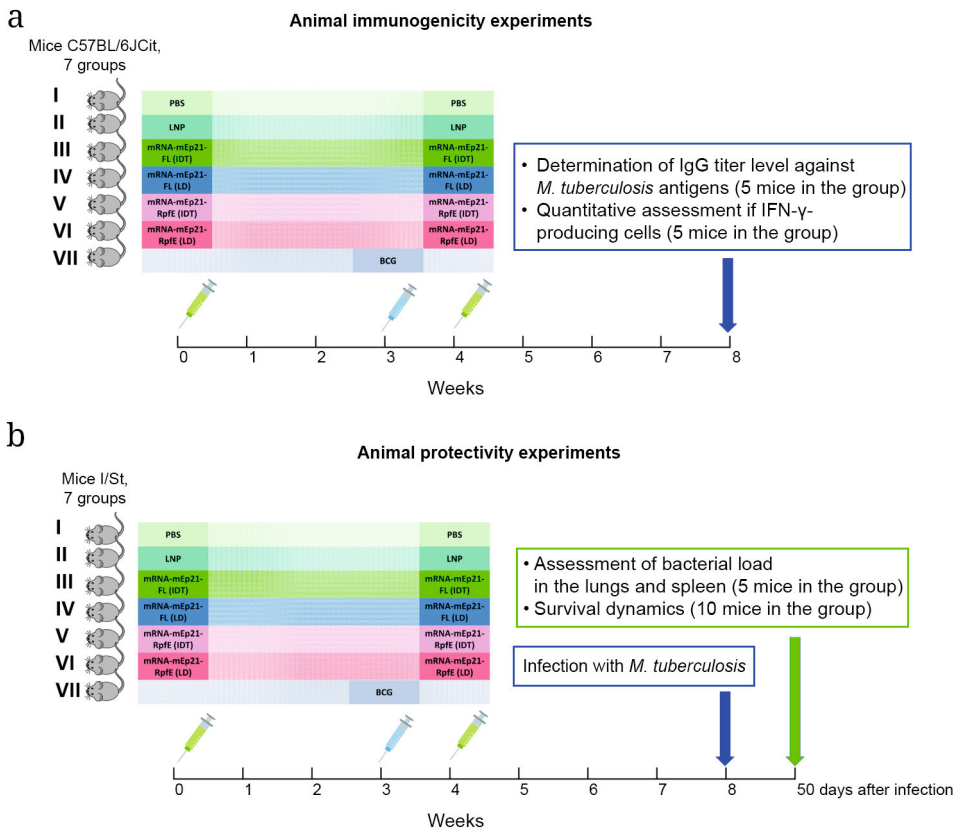

Fig. 3. Design of the *in vivo* experiments. a) Evaluation of the vaccine immunogenicity in B6 mice; b) Evaluation of the vaccine protective properties in I/St mice.

proteasomal degradation and presentation in the content of MHC I. We also used two adjuvant sequences (RpfE from *M. tuberculosis* and human FL). After designing the amino acid sequences of the vaccines, we applied two cardinally different optimization algorithms, IDT and LD, to obtain four mRNA sequences (mRNA-mEp21-RpfE-IDT, mRNA-mEp21-FL-IDT, mRNA-mEp21-RpfE-LD, and mRNA-mEp21-FL-LD). All mRNAs contained a set of essential mRNA elements, such as the cap, 5′ and 3′ UTRs, and the polyA tail of 110 adenine residues.

The designed mRNAs were synthesized, encapsulated into LNPs, and injected into mice for testing their immunogenicity and protective efficacy against *M. tuberculosis* infection. The full workflow of the study is presented in Fig. 3.

The target *M. tuberculosis* proteins that play a key role in the infection, associated pathological process, and induction of a strong immune response, were selected based on our recent systematic review of vaccines against *M. tuberculosis* [26]. We selected the most commonly used *M. tuberculosis* antigens: ESAT6 (WGG95196.1), CFP10 (WGG95197.1), Ag85B (WP_262239103.1), Ag85A (P9WQP3.1), HspX (CCE37510.1), MPT83 (ANZ83596.1), PE/PPE family proteins PPE55 (VCU51654.1) and PPE68 (CCE39296.1, SGL17895.1, CNN07764.1, and AAC32213.1), Mtb8.4 (CAA15851), Rv1733c (P9WLS9.1), MPT64 (CAA53143.1), and Hrp1 (CCP45424.1). ESAT6 and CFP10 are the low-molecular-weight secretory proteins that are important for the mycobacterial virulence and pathogenicity and encoded by genes of the *RD1* locus, which is absent in the BCG [66, 67]. The secreted proteins Ag85A and Ag85B, which bind fibronectin and have the mycolyltransferase activity, are essential for maintaining the integrity of the mycobacterial cell wall. The HspX chaperone is a dominant antigen produced by *M. tuberculosis* at the latent infection stage; it is thought to enhance the long-term stability of proteins and cellular structures, thereby helping the tuberculosis pathogen to survive for a long time [68, 69]. MPT83 is a glycosylated lipoprotein found on the surface of mycobacterial cells that evokes a strong T-cell response and antibody production [70]. Proteins of the PE/PPE family are characterized by the presence of conserved Pro-Glu (PE) and Pro-Pro-Glu (PPE) motifs in their N-terminal regions, respectively; they induce activation of B and T cells and modulate the host's immune response [71]. Mtb8.4 is an immunoreactive antigen for T cells and is found in humans with latent mycobacterial infections; it induces high levels of IFN-γ (Th1 cytokine) secretion [72]. Rv1733c is the

main latency antigen of *M. tuberculosis*; it is actively expressed by latent *M. tuberculosis* cells and is well recognized by T cells of infected individuals [73]. MPT64 promotes the antituberculosis cellular immunity and activates macrophages, thus inducing secretion of IL-1β, IL-6, IL-10, and TNF-α by these cells. MPT64 can also partially inhibit the apoptosis in macrophages [74]. HRP1 is a secreted protein encoded by the *DosR* locus and has a strong antigenic activity [75, 76].

Prediction and evaluation of LBL, CTL, and HTL epitopes. Using the ABCpred online server, we obtained 448 LBL epitopes. Their analysis in VaxiJen, ToxinPred, AllerTOP 2.0, and BLAST yielded 185 antigenic, nontoxic, and nonallergenic epitopes with no homology to human and mouse sequences. From these, we selected seven most antigenic epitopes. According to the IgPred server, none of these epitopes stimulated IgE production; at the same time, all epitopes exhibited a high similarity to the epitopes inducing IgG production.

Using the T Cell Prediction Class I service, 18,547 CTL epitopes were obtained for all the studied antigens; 176 epitopes demonstrating the best binding to MHC I were chosen for further analysis. Their assessment with VaxiJen produced 126 epitopes proven to be antigenic with an over 66% probability. According to ToxinPred, 125 of them were nontoxic, and among these, 72 epitopes were identified as nonallergenic by AllerTOP 2.0. Analysis for the homology with human and mouse sequences limited this number to 70 epitopes, from which seven most antigenic epitopes were selected (the probability of the selected epitopes being antigens was 100%, based on the verification by the VaxiJen v3.0 service) and used for construction of the vaccine proteins and molecular docking with MHC I.

Using the MHC-II Binding Predictions service, 150,000 HTL epitopes were found in all antigen sequences. After all necessary checks, 192 HTL epitopes were selected, which were assessed for their ability to induce the production of IFN-γ, IL-4, and IL-10. Given that IFN-γ is a key cytokine in the antituberculosis response, we mostly selected the epitopes capable of inducing the synthesis of this protein. On the other hand, induction of the anti-inflammatory cytokines IL-4 and IL-10 positively correlates with the increase in the *M. tuberculosis* load and, therefore, is undesirable. Accordingly, only HTL epitopes that presumably did not induce the expression of these two cytokines were used in our research. Seven most antigenic epitopes (100% probability of being antigens based on the verification by the VaxiJen v3.0 service) were utilized for the construction of the vaccine protein and molecular docking with MHC II. More detailed information on the selected epitopes is presented in Table S1 in Online Resource 2.

Molecular docking between T-lymphocyte epitopes and MHC alleles. The results of the HLA protein docking with CTL and HTL epitopes are presented in Fig. S1 in Online Resource 2. The best RMSD and binding free energy values for MHC I were found for the interaction between the AGNFERISGD epitope and HLA-A*24:02. For MHC II, the best parameters were found for the GLLDPSQAMGPTLIG epitope interaction with HLA-DRB1*15:01 (Fig. S2 in Online Resource 2). For 4 out of 7 CTL epitopes, the RMSD was less than 3 Å, implying a high probability of interaction with MHC I. Among the HTL epitopes, six peptides out of seven had the RMSD values < 3 Å. Nevertheless, we decided to include all the studied epitopes in the vaccine, since these epitopes had been predicted to interact with other MHC alleles other than alleles used for the docking procedure, although this interaction could not be confirmed by docking because of the absence of corresponding 3D structures in the databases. It is likely that the docking results obtained for such alleles and their epitopes could be even more acceptable than those presented in this article. Moreover, the docking with MHC I and MHC II was only one of the ways to assess the quality of the epitopes used in our study. Moreover, the other parameters demonstrated by the epitopes with less acceptable RMSD values were comparable to the values exhibited by the epitopes with "good" RMSD, therefore, we did not exclude them from the study.

Prediction of antigenicity, allergenicity, toxicity, and physicochemical properties of the vaccine proteins. The amino acid sequences of the vaccine proteins were tested for antigenicity, allergenicity, and toxicity using the VaxiJen, ANTIGENpro, AllerTOP, and ToxinPred servers. Both mRNA-mEp21-FL and mRNA-mEp21-RpfE vaccines types were found to be antigenic, nonallergenic, nontoxic, and stable, with II < 40 (conventional units of this server). The mRNA-mEp21-FL vaccine was also thermally stable; the GRAVY parameter was < 0 for both vaccine types, indicating the hydrophilicity of the resulting constructs (Table S2 in Online Resource 2).

Determination and confirmation of the tertiary structure of vaccine proteins. The tertiary structure was obtained with the Robetta server. Because Robetta offered five models for each construct, we used PROCHECK to select a model with the best stereochemical accuracy for further work (Table S3 in Online Resource 2). The best models are presented in Fig. S3 in Online Resource 2.

Prediction of B-cell conformational epitopes. The formation of the tertiary structure gives rise to B-cell conformational epitopes, which were predicted using the ElliPro server. The evaluation of discontinuous conformational epitopes is presented in Table S4 in Online Resource 2. In mRNA-mEp21-FL,

294 a.a. were found in the conformational B-epitopes with the predicted values from 0.915 to 0.56 (conventional units ranging from 0 to 1 showing how much an isolated epitope "protrudes" beyond the average boundaries of the protein represented as an ellipsoid; larger values indicate that the protein region is more likely to protrude outward, i.e., likely to act as a B cell epitope). In mRNA-mEp21-RpfE, 269 a.a. were found with the predicted values from 0.861 to 0.527. In the RpfE-containing vaccine protein, the bulk of the adjuvant and most of the LBL and CTL epitopes turned out to be B-cell conformational epitopes. By contrast, in the FL-containing vaccine protein, the conformational epitopes were mostly HTL and LBL epitopes. The 2D and 3D models of the B-cell conformational epitopes in the vaccine proteins are shown in Figs. S4-S6 in Online Resource 2.

Molecular docking of the vaccine proteins with TLR4. The affinity of the mEp21-RpfE and mEp21-FL proteins toward TLR4 was comparable to that of RpfE, which is expected to stimulate an immune response against *M. tuberculosis* (Table S5 in Online Resource 2). The hypothetical interactions of the TLR4 complex with the mEp21-RpfE and mEp21-FL proteins (Fig. S7 in Online Resource 2) were examined on the PDBsum server (Fig. S8 in Online Resource 2). The results of molecular docking indicated that the vaccine proteins presumably have an affinity for TLR4 that is similar to the affinity of RpfE, as well as possess comparable adjuvant characteristics.

***In silico* immunization.** The used model included three injections of each investigated vaccine to simulate the immune response, and produced similar predicted immune responses for all the tested vaccines (Fig. S9 in Online Resource 2). The modeling results implied a higher extent of IgM induction as compared to IgG. Furthermore, after a decrease in the vaccine antigen level, the content the immunoglobulins remained high, and the number of memory B cells increased, possibly indicating formation of the immune memory after exposure to the antigen. The emergence of memory cells and active Tc (T cytotoxic) lymphocytes among the Th (T helper) and Tc cell populations, respectively, was possible. The levels of IFN-γ and IL-2 (important cytokines involved in the progression of immune response against tuberculosis) were also predicted to increase after the immunization. The Simpson index (D) remained low during the entire period of *in silico* immunization, implying a potential production of interleukins and cytokines. Therefore, the results of *in silico* modeling demonstrated that all variants of the developed vaccines were presumably effective and safe.

Optimization of codon composition and removal of miRNA-binding sites. The employed optimization algorithms (Linear Design, RiboTree, IDT, genewiz, and iCodon) were compared with each other via the Superfolder algorithm (Fig. S10 in Online Resource 2). Comparison of the key parameters of mRNA stability and translatability allowed us to select two optimization algorithms: Linear Design and IDT. According to the results of *in silico* analysis, optimization with Linear Design considerably extended the half-life of RNA, suggesting mRNA stabilization and a hypothetical increase in the number of synthesized protein molecules. However, Linear Design showed a low AUP init 14 value, which could potentially diminish the translational efficiency, as low AUP values could slow down the movement of ribosomes along the highly structured RNA molecule. The IDT algorithm yielded higher AUP and AUP init 14 values, presumably affecting the availability of mRNA for protein synthesis. Various optimization algorithms were applied to each vaccine protein. As a result, four mRNA sequences were developed: mRNA-mEp21-RpfE-LD, mRNA-mEp21-FL-LD, mRNA-mEp21-RpfE-IDT, and mRNA-mEp21-FL-IDT (Fig. 4). The stability characteristics of the four mRNA vaccine sequences are presented in Fig. S11 in Online Resource 2.

We also removed the miRNA-binding sites from all four constructs, because of the ability of such sites causing RNA interference and translation inhibition. The final secondary structures of all four full-length mRNAs obtained using RNAfold (http://rna.tbi.univie.ac.at/cgi-bin/RNAWebSuite/RNAfold.cgi) are presented in Fig. 4. As one can see, the sequences obtained with the Linear Design algorithm are much more structured than the sequences obtained with IDT.

The efficacy of the developed mRNA vaccines in *in vivo* experiments. To evaluate the immunogenicity of the antituberculosis multiepitope mRNA-mEp21 vaccines in B6 mice, we quantified the cellular and humoral immune responses to the mycobacterial antigens. The cellular response was assessed by the ELISpot assay, and the humoral immunity was determined as the titers of IgG antibodies to mycobacterial antigens from the *M. tuberculosis* sonicate.

After immunization, there were differences in the number of IFN-γ-producing cells between the mouse groups [ANOVA: $F(6, 28) = 11.58$, $p < 0.001$]. Thus, the number of IFN-γ-producing cell increased only in animals immunized with mRNA-mEp21-RpfE-LD and BCG compared to the control group ($p = 0.042$ and 0.012, respectively; Fig. 5a). Hence, only one of the developed mRNA vaccines ensured the induction of cellular immunity against *M. tuberculosis* antigens, and this response was less pronounced compared to the immunization with BCG.

Immunization induced a significant increase in the titers of IgG antibodies against mycobacterial antigens at four serum dilutions: 1 : 50, 1 : 100, 1 : 200, and 1 : 400 [ANOVA, 1 : 50: $F(6, 28) = 13.23$, $p < 0.0001$;

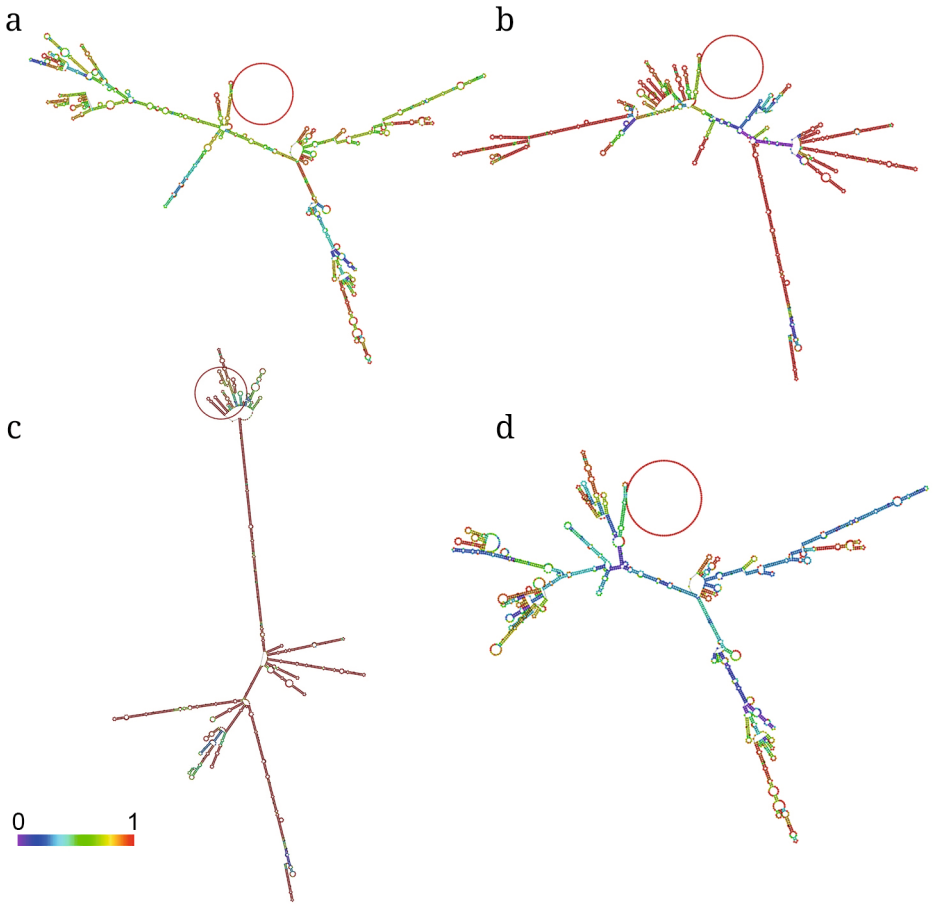

Fig. 4. Secondary MFE (minimum free energy) structures of vaccine mRNAs. a) mRNA-mEp21-RpfE (Linear Design); b) mRNA-mEp21-RpfE (IDT); c) mRNA-mEp21-FL (Linear Design); d) mRNA-mEp21-FL (IDT). The color scale indicates the probability of base pairing, where 0 is the minimal probability and 1 is the maximal probability.

1 : 100: $F(6, 28) = 16.31$, $p < 0.001$; 1 : 200: $F(6, 28) = 10.91$, $p < 0.001$; 1 : 400: $F(6, 28) = 10,62$, $p < 0.001$]. The maximum serum titer at which significant differences were observed between the mice receiving the vaccine and the negative control group was 1 : 50 for mRNA-mEp21-FL-IDT, 1 : 100 for mRNA-mEp21-FL-LD, 1 : 200 for mRNA-mEp21-RpfE-IDT, and 1 : 400 for mRNA-mEp21-RpfE-LD (Fig. 5d). Moreover, no significant differences were found among different mRNA vaccines. On the other hand, immunization with BCG produced higher IgG titers. Therefore, immunization with experimental mRNA vaccines led to the formation of the humoral IgG immune response to mycobacterial antigens at all four serum dilutions. However, similar to the cellular immune response, the induced immunity was manifested less compared to the vaccination with BCG.

To assess the protective properties of the mRNA vaccines, prophylactically immunized I/St mice were infected with *M. tuberculosis*, and the mycobacterial load in their lungs and spleen was determined 50 days after the infection. We found that immunization affected the bacterial loads in the lungs and spleen [$F(6, 28) = 4.807$, $p = 0.01$, and $F(6, 28) = 10.28$, $p < 0.001$]. In the lungs, both BCG and mRNA-mEp21-FL-IDT decreased the bacterial load ($p < 0.001$ and $p = 0.002$, respectively, Fig. 5b), whereas in the spleen, the reduction in the bacterial load was observed only after vaccination with BCG ($p = 0.011$). Immunization with any mRNA vaccine did not significantly lower the bacterial load in the spleen, even in the case of mRNA-mEp21-FL-IDT ($p = 0.105$, Fig. 5c). Administration of mRNA-mEp21-FL-IDT diminished the number of CFU by 79.37% (0.686 $\log_{10}$ units) in the lungs and by 86.2% (0.86 $\log_{10}$ units) in the spleen, whereas BCG reduced the number of CFU in the lungs by 90.6% (1.025 $\log_{10}$ units) and by 80.4% in the spleen (0,708 $\log_{10}$ units).

Mouse survival after infection with *M. tuberculosis* was evaluated on day 111 after the infection (Fig. 5e). In the control group (mice that received PBS), eight out of 10 animals had died by the end of the experiment, whereas in the BCG and mRNA-mEp21-FL-IDT groups, only two mice out of 10 had died. The Kaplan–Meier survival analysis revealed a significant extension of the lifespan of mice vaccinated

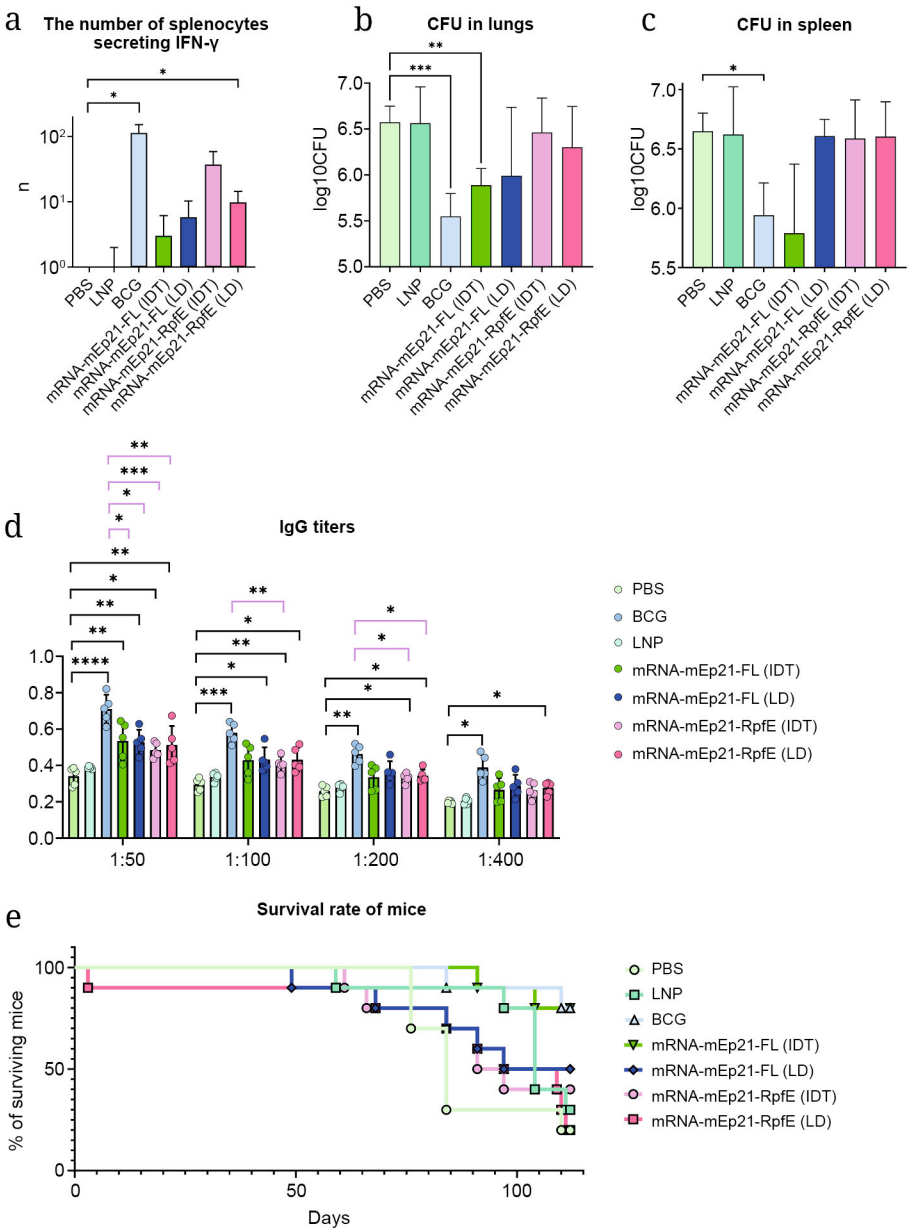

Fig. 5. *In vivo* experiments. The number of splenocytes secreting IFN-γ, IgG titers, CFU in the lungs and spleen (n = 5 mice per group), and survival after infection (n = 10 mice per group) were evaluated. a) Estimation of the number of cells secreting IFN-γ in response to the stimulation with *M. tuberculosis* antigens by the ELISpot assay; b and c) evaluation of the bacterial load in the (b) lungs and (c) spleen (the number of *M. tuberculosis* CPUs in the tissue homogenate 50 days after infection); d) IgG titers in response to the stimulation with *M. tuberculosis* antigens; e) survival of mice after infection with *M. tuberculosis*; * $p < 0.05$; ** $p < 0.01$; *** $p < 0.001$; **** $p < 0.0001$.

with BCG or mRNA-mEp21-FL-IDT as compared to animals of the control group (Mantel–Cox log-rank test, $p = 0.0011$). It should be noted that the weight loss dynamics in mice of the mRNA-mEp21-FL-IDT group was similar to that in the BCG group (data not shown).

Overall, our results showed that despite inducing a less pronounced adaptive response, the mRNA-mEp21-FL-IDT mRNA vaccine provided efficient protection (comparable with that of BCG) after a challenge with *M. tuberculosis*.

DISCUSSION

Here, we used immunoinformatic methods to develop a new multiepitope antituberculosis mRNA vaccine encoding 21 epitopes from 11 proteins of *M. tuberculosis*. We also used the sequences of molecular adjuvants RpfE and FL and employed two strategies for optimizing the secondary structure of the RNA molecule (Linear Design and IDT), which allowed us to obtain four mRNA vaccines, which efficacy

was tested in mice. All the developed vaccines induced humoral immunity against *M. tuberculosis* antigens, which corresponded to the results of *in silico* immunization. On the other hand, only the mRNA-mEp21-RpfE-IDT vaccine induced the cellular immunity, which is at odds with the data obtained by *in silico* immunization. According to these data, vaccines with the RpfE adjuvant should cause weaker cellular immunity compared to vaccines with the FL adjuvant, since the former is less likely to stimulate the maturation of cytotoxic T-lymphocytes. In our experiments, the most efficient protection against tuberculosis was provided by the mRNA-mEp21-FL-IDT vaccine containing the FL molecular adjuvant. Our results have shown that the two-dose (5 μg each dose) immunization with RNA-mEp21-FL-IDT reduced the mycobacterial load in the lungs and increased the animal survival rate to 80%, which was comparable to the efficacy of the BCG vaccine.

The observed differences in the effects of the incorporated molecular adjuvants may be explained by their functions. The FL sequence has been widely used in the vaccines against the pseudorabies virus, simian immunodeficiency virus, etc., as well as in cancer immunotherapy [77-79]. FL mobilizes and stimulates DCs, natural killer cells, and B cells. Its inclusion in the DNA vaccines enhances the immune response [80-82]. In our work, the FL-based vaccine induced the humoral response and the protective immunity, but the cellular response was modest (less than 12 IFN-γ spots per well). In other studies on the development of DNA vaccines against tuberculosis, incorporation of the FL sequence has caused more pronounced formation of both humoral response (as judged by the IgG titer) and cellular response (as evidenced by the elevated production of IFN-γ by splenocytes after their specific activation), as well as caused a more significant decline in the mycobacterial load in the lungs and spleen (although this effect was still less pronounced compared with the BCG vaccine) [17, 83-85]. In most of research articles, however, the efficacy of antituberculosis DNA vaccines has been inferior to that of BCG [26].

RpfE is a *M. tuberculosis* protein that is an agonist of TLR4. TLR4 plays an important role in the protection against tuberculosis: the knockout of the *TLR4* gene leads to the increase in the bacterial load in infected mice [86]. In our study, incorporation of the RpfE sequence ensured a more pronounced formation of cellular immunity but did not ensure the protection of the animals after the infection. Similarly to our findings, Xin et al. [87] showed that the inclusion of RpfE strengthened the cellular immunity against *M. tuberculosis* but did not reduce the bacterial load in the infected animals. We believe that the lack of the protective effect may be due to the excessive immunogenicity of the adjuvant and to the development of systemic inflammation after its administration. Thus, we observed spleen enlargement, inflammation at the injection site, and intestinal inflammation in some mice of the mRNA-mEp21-RpfE group (data not shown). However, no negative effects of RpfE have been observed in other studies of this adjuvant [88, 89].

A distinctive feature of our work is application of two cardinally different algorithms (LD and IDT) for optimizing the RNA secondary structure. Presumably, LD promotes an increase in the RNA lifetime and decreases the number of unpaired bases, whereas IDT ensures the balanced codon use and allows to avoid rare codons. We did not find significant differences in the efficacy of mRNA vaccines developed with different optimization algorithms, although it has been reported earlier that the LD algorithm notably enhanced the humoral immune response in mice after administration of mRNA vaccines against COVID-19 and chickenpox virus [58].

Overall, we used immunoinformatic methods to create a multiepitope antituberculosis vaccine, mRNA-mEp21-FL-IDT, which induced the humoral immunity and reduced bacterial load in the lungs, while improving animal survival after infection with *M. tuberculosis* with the efficiency comparable to that of the BCG vaccine. However, the results of our work do not allow to conclude about the efficacy of the adjuvants or optimization algorithms. In our previous studies, the developed multiepitope mRNA antituberculosis vaccines encoding five epitopes of the immunodominant protein ESAT6 (MTB-mEp-5-1 and mEpitope-ESAT6) were highly immunogenic, but their protective properties were worse than those of BCG [90, 91]. Other articles on the design of antituberculosis DNA and RNA vaccines also indicate that in most cases, the vaccines induced the adaptive immunity but failed to protect from *M. tuberculosis* infection [10, 26]. Moreover, even when the protective response was successfully induced, only in rare cases immunization with nucleic acid-based antituberculosis vaccines provided a stronger protection compared to BCG [26]. In this context, the most efficient DNA vaccines have been those encoding the ESAT6, CFP10, CFP21, MTP64, Ag85B, or MPT63 antigens [17, 92, 93]. Among them, ESAT6 provided the best protection, while the addition of the adjuvant (FL, IL-12, or IL-23) has further reduced the number of CFU.

In conclusion, here we combined for the first time the multiepitope design of an mRNA vaccine, inclusion of molecular adjuvant sequence, and RNA sequence optimization, which allowed us to obtain an effective antituberculosis mRNA vaccine (mRNA-mEp21-FL-IDT) with a protective effect against *M. tuberculosis* infection. The efficacy and safety of mRNA-mEp21-FL-IDT should be confirmed in expanded preclinical studies.

Abbreviations. AUP, average unpaired probability; BCG, Bacillus Calmette–Guérin vaccine; CFU, colony-forming unit; CTL, cytotoxic T lymphocyte; DC, dendritic cell; FL, FMS-like tyrosine kinase-3 ligand; HLA, human leukocyte antigens; HTL, helper T lymphocyte; LBL, linear B lymphocyte; LNP, lipid nanoparticle; MHC, major histocompatibility complex; MITD, MHC I-targeting domain; RMSD, root-mean-square distance; RpfE, resuscitation-promoting factor; TLR, Toll-like receptor; tPA, tissue plasminogen activator; UTR, untranslated region.

Supplementary information. The online version contains supplementary material available at https://doi.org/10.1134/S0006297925600073.

Acknowledgments. The authors are grateful to O. V. Zaborova (Lomonosov Moscow State University) for her assistance with the mRNA encapsulation into LNPs. Equipment from the Resource Centers for genetic engineering and biotechnological products at the Sirius University of Science and Technology was used in the study.

Contributions. A.A.K., I.S.K., and V.V.R. developed the genetic constructs, produced the plasmids, prepared mRNAs, and wrote the manuscript; R.A.I. and V.V.R. developed the study concept, supervised the research, discussed the results, and edited the manuscript; G.S.Sh. and V.V.E. conducted *in vivo* experiments and edited the manuscript.

Funding. The project was supported by the Ministry of Science and Higher Education of the Russian Federation (Agreement no. 075-10-2025-017).

Ethics approval and consent to participate. The animal study protocol was approved by the Ethics Committee of the Central Tuberculosis Research Institute (protocol no. 3/2; May 11, 2023) in accordance with the EU Directive 2010/63/EU on animal experiments and was implemented in accordance with the European Convention ETS no. 123 for the Protection of Vertebrate Animals used for Experimental or Scientific Purposes (Strasbourg) (1986, with the 2006 amendment), the International Agreement on Humane Treatment of Animals (1986), and the Guide for the Care and Use of Laboratory Animals, 8th ed. (2010).

Conflict of interest. The authors of this work declare that they have no conflicts of interest.

REFERENCES

1. Global tuberculosis report 2024 (2024) URL: https://www.who.int/teams/global-programme-on-tuberculosis-and-lung-health/tb-reports/global-tuberculosis-report-2024.
2. Colditz, G. A., Brewer, T. F., Berkey, C. S., Wilson, M. E., Burdick, E., Fineberg, H. V., and Mosteller, F. (1994) Efficacy of BCG vaccine in the prevention of tuberculosis. Meta-analysis of the published literature, *JAMA*, **271**, 698-702, https://doi.org/10.1001/jama.1994.03510330076038.
3. Gandhi, R. T., Kwon, D. S., Macklin, E. A., Shopis, J. R., McLean, A. P., McBrine, N., Flynn, T., Peter, L., Sbrolla, A., Kaufmann, D. E., Porichis, F., Walker, B. D., Bhardwaj, N., Barouch, D. H., and Kavanagh, D. G. (2016) Immunization of HIV-1-infected persons with autologous dendritic cells transfected with mRNA encoding HIV-1 Gag and Nef: results of a randomized, placebo-controlled clinical trial, *J. Acquir Immune Defic.*, **71**, 246-253, https://doi.org/10.1097/QAI.0000000000000852.
4. Richner, J. M., Himansu, S., Dowd, K. A., Butler, S. L., Salazar, V., Fox, J. M., Julander, J. G., Tang, W. W., Shresta, S., Pierson, T. C., Ciaramella, G., and Diamond, M. S. (2017) Modified mRNA vaccines protect against Zika virus infection, *Cell*, **6**, 1114-1125, https://doi.org/10.1016/j.cell.2017.02.017.
5. Alberer, M., Gnad-Vogt, U., Hong, H. S., Mehr, K. T., Backert, L., Finak, G., Gottardo, R., Bica, M. A., Garofano, A., Koch, S. D., Fotin-Mleczek, M., Hoerr, I., Clemens, R., and von Sonnenburg, F. (2017) Safety and immunogenicity of a mRNA rabies vaccine in healthy adults: an open-label, non-randomised, prospective, first-in-human phase 1 clinical trial, *Lancet*, **390**, 1511-1520, https://doi.org/10.1016/S0140-6736(17)31665-3.
6. Bahl, K., Senn, J. J., Yuzhakov, O., Bulychev, A., Brito, L. A., Hassett, K. J., Laska, M. E., Smith, M., Almarsson, Ö., Thompson, J., Ribeiro, A. M., Watson, M., Zaks, T., and Ciaramella, G. (2017) Preclinical and clinical demonstration of immunogenicity by mRNA vaccines against H10N8 and H7N9 influenza viruses, *Mol. Ther.*, **6**, 1316-1327, https://doi.org/10.1016/j.ymthe.2017.03.035.
7. Pateev, I., Seregina, K., Ivanov, R., and Reshetnikov, V. (2023) Biodistribution of RNA vaccines and of their products: evidence from human and animal studies, *Biomedicines*, **12**, 59, https://doi.org/10.3390/biomedicines12010059.
8. Hu, C., Bai, Y., Liu, J., Wang, Y., He, Q., Zhang, X., Cheng, F., Xu, M., Mao, Q., and Liang, Z. (2024) Research progress on the quality control of mRNA vaccines, *Expert Rev. Vaccines*, **23**, 570-583, https://doi.org/10.1080/14760584.2024.2354251.
9. Fan, X. Y., and Lowrie, D. B. (2021) Where are the RNA vaccines for TB? *Emerg. Microbes Infect.*, **10**, 1217-1218, https://doi.org/10.1080/22221751.2021.1935328.
10. Khlebnikova, A., Kirshina, A., Zakharova, N., Ivanov, R., and Reshetnikov, V. (2024) Current progress in the development of mRNA Vaccines against bacterial infections, *Int. J. Mol. Sci.*, **25**, 13139, https://doi.org/10.3390/ijms252313139.
11. Cianci, R., and Franza, L. (2022) Recent advances in vaccine technology and design, *Vaccines (Basel)*, **10**, 624, https://doi.org/10.3390/vaccines10040624.

12. Zhang, L. (2018) Multi-epitope vaccines: a promising strategy against tumors and viral infections, *Cell. Mol. Immunol.*, **15**, 182-184, https://doi.org/10.1038/cmi.2017.92.
13. Mahapatra, S. R., Dey, J., Kaur, T., Sarangi, R., Bajoria, A. A., Kushwaha, G. S., Misra, N., and Suar, M. (2021) Immunoinformatics and molecular docking studies reveal a novel multi-epitope peptide vaccine against pneumonia infection, *Vaccine*, **39**, 6221-6237, https://doi.org/10.1016/j.vaccine.2021.09.025.
14. Dey, J., Mahapatra, S. R., Lata, S., Patro, S., Misra, N., and Suar, M. (2022) Exploring Klebsiella pneumoniae capsule polysaccharide proteins to design multiepitope subunit vaccine to fight against pneumonia, *Expert Rev. Vaccines*, **21**, 569-587, https://doi.org/10.1080/14760584.2022.2021882.
15. Dey, J., Mahapatra, S. R., Patnaik, S., Lata, S., Kushwaha, G. S., Panda, R. K., Misra, N., and Suar, M. (2022) Molecular characterization and designing of a novel multiepitope vaccine construct against *Pseudomonas aeruginosa*, *Int. J. Pept. Res. Ther.*, **28**, 49, https://doi.org/10.1007/s10989-021-10356-z.
16. Alharbi, M., Alshammari, A., Alasmari, A. F., Alharbi, S. M., Tahir Ul Qamar, M., Ullah, A., Ahmad, S., Irfan, M., and Khalil, A. A. K. (2022) Designing of a recombinant multi-epitopes based vaccine against *Enterococcus mundtii* using bioinformatics and immunoinformatics approaches, *Int. J. Environ. Res. Public Health*, **19**, 3729, https://doi.org/10.3390/ijerph19063729.
17. Jiang, Q., Zhang, J., Chen, X., Xia, M., Lu, Y., Qiu, W., Feng, G., Zhao, D., Li, Y., He, F., Peng, G., and Wang, Y. (2013) A novel recombinant DNA vaccine encoding Mycobacterium tuberculosis ESAT-6 and FL protects against Mycobacterium tuberculosis challenge in mice, *J. Biomed. Res.*, **5**, 406-420, https://doi.org/10.7555/JBR.27.20120114.
18. Choi, H. G., Kim, W. S., Back, Y. W., Kim, H., Kwon, K. W., Kim, J. S., Shin, S. J., and Kim, H. J. (2015) Mycobacterium tuberculosis RpfE promotes simultaneous Th1- and Th17-type T-cell immunity via TLR4-dependent maturation of dendritic cells, *Eur. J. Immunol.*, **45**, 1957-1971, https://doi.org/10.1002/eji.201445329.
19. Jung, I. D., Jeong, S. K., Lee, C. M., Noh, K. T., Heo, D. R., Shin, Y. K., Yun, C. H., Koh, W. J., Akira, S., Whang, J., Kim, H. J., Park, W. S., Shin, S. J., and Park, Y. M. (2011) Enhanced efficacy of therapeutic cancer vaccines produced by co-treatment with Mycobacterium tuberculosis heparin-binding hemagglutinin, a novel TLR4 agonist, *Cancer Res.*, **71**, 2858-2870, https://doi.org/10.1158/0008-5472.CAN-10-3487.
20. Lee, S. J., Shin, S. J., Lee, M. H., Lee, M. G., Kang, T. H., Park, W. S., Soh, B. Y., Park, J. H., Shin, Y. K., Kim, H. W., Yun, C. H., Jung, I. D., and Park, Y. M. (2014) A potential protein adjuvant derived from *Mycobacterium tuberculosis* Rv0652 enhances dendritic cells-based tumor immunotherapy, *PLoS One*, **9**, e104351, https://doi.org/10.1371/journal.pone.0104351.
21. Gote, V., Bolla, P. K., Kommineni, N., Butreddy, A., Nukala, P. K., Palakurthi, S. S., and Khan, W. (2023) A comprehensive review of mRNA vaccines, *Int. J. Mol. Sci.*, **24**, 2700, https://doi.org/10.3390/ijms24032700.
22. Muslimov, A., Tereshchenko, V., Shevyrev, D., Rogova, A., Lepik, K., Reshetnikov, V., and Ivanov, R. (2023) The dual role of the innate immune system in the effectiveness of mRNA therapeutics, *Int. J. Mol. Sci.*, **24**, 14820, https://doi.org/10.3390/ijms241914820.
23. Mauger, D. M., Cabral, B. J., Presnyak, V., Su, S. V., Reid, D. W., Goodman, B., Link, K., Khatwani, N., Reynders, J., Moore, M. J., and McFadyen, I. J. (2019) mRNA structure regulates protein expression through changes in functional half-life, *Proc. Natl. Acad. Sci. USA*, **116**, 24075-24083, https://doi.org/10.1073/pnas.1908052116.
24. Wayment-Steele, H. K., Kim, D. S., Choe, C. A., Nicol, J. J., Wellington-Oguri, R., Watkins, A. M., Parra Sperberg, R. A., Huang, P. S., Participants, E., and Das, R. (2021) Theoretical basis for stabilizing messenger RNA through secondary structure design, *Nucleic Acids Res.*, **49**, 10604-10617, https://doi.org/10.1093/nar/gkab764.
25. María, R. R., Arturo, C. J., Alicia, J. A., Paulina, M. G., and Gerardo, A. O. (2017) The impact of bioinformatics on vaccine design and development, *InTech*, https://doi.org/10.5772/intechopen.69273.
26. Kazakova, A., Zhelnov, P., Sidorov, R., Rogova, A., Vasileva, O., Ivanov, R., Reshetnikov, V., and Muslimov, A. (2024) DNA and RNA vaccines against tuberculosis: a scoping review of human and animal studies, *Front. Immunol.*, **15**, 1457327, https://doi.org/10.3389/fimmu.2024.1457327.
27. Yang, Y., Chen, Y. Z., and Xia, T. (2024) Optimizing antigen selection for the development of tuberculosis vaccines, *Cell Insight*, **3**, 100163, https://doi.org/10.1016/j.cellin.2024.100163.
28. Saha, S., and Raghava, G. P. (2006) Prediction of continuous B-cell epitopes in an antigen using recurrent neural network, *Proteins*, **1**, 40-48, https://doi.org/10.1002/prot.21078.
29. Saha, S., and Raghava, G. P. S. (2004) BcePred: prediction of continuous B-Cell epitopes in antigenic sequences using physico-chemical properties, *Lecture Notes Comput. Sci.*, **3239**, 197-204, https://doi.org/10.1007/978-3-540-30220-9_16.
30. Fleri, W., Paul, S., Dhanda, S. K., Mahajan, S., Xu, X., Peters, B., and Sette, A. (2017) The immune epitope database and analysis resource in epitope discovery and synthetic vaccine design, *Front. Immunol.*, **8**, 278, https://doi.org/10.3389/fimmu.2017.00278.
31. Johnson, M., Zaretskaya, I., Raytselis, Y., Merezhuk, Y., McGinnis, S., and Madden, T. L. (2008) NCBI BLAST: a better web interface, *Nucleic Acids Res.*, **36**, W5-W9, https://doi.org/10.1093/nar/gkn201.

32. Doytchinova, I. A., and Flower, D. R. (2007) VaxiJen: a server for prediction of protective antigens, tumour antigens and subunit vaccines, *BMC Bioinform.*, **8**, 4, https://doi.org/10.1186/1471-2105-8-4.
33. Dimitrov, I., Bangov, I., Flower, D. R., and Doytchinova, I. (2014) AllerTOP v. 2 – a server for *in silico* prediction of allergens, *J. Mol. Model*, **20**, 2278, https://doi.org/10.1007/s00894-014-2278-5.
34. Sharma, N., Naorem, L. D., Jain, S., and Raghava, G. P. S. (2022) ToxinPred2: an improved method for predicting toxicity of proteins, *Brief. Bioinform.*, **23**, bbac174, https://doi.org/10.1093/bib/bbac174.
35. Gupta, S., Ansari, H. R., Gautam, A., Open Source Drug Discovery Consortium, and Raghava, G. P. (2013) Identification of B-cell epitopes in an antigen for inducing specific class of antibodies, *Biol. Direct.*, **8**, 27, https://doi.org/10.1186/1745-6150-8-27.
36. Dhanda, S. K., Vir, P., and Raghava, G. P. (2013) Designing of interferon-gamma inducing MHC class-II binders, *Biol. Direct.*, **8**, 30, https://doi.org/10.1186/1745-6150-8-30.
37. Dhanda, S. K., Gupta, S., Vir, P., and Raghava, G. P. (2013) Prediction of IL4 inducing peptides, *Clin. Dev. Immunol.*, **2013**, 263952, https://doi.org/10.1155/2013/263952.
38. Nagpal, G., Usmani, S. S., Dhanda, S. K., Kaur, H., Singh, S., Sharma, M., and Raghava, G. P. (2017) Computer-aided designing of immunosuppressive peptides based on IL-10 inducing potential, *Sci. Rep.*, **7**, 42851, https://doi.org/10.1038/srep42851.
39. Bui, H. H., Sidney, J., Dinh, K., Southwood, S., Newman, M. J., and Sette, A. (2006) Predicting population coverage of T-cell epitope-based diagnostics and vaccines, *BMC Bioinformatics*, **7**, 153, https://doi.org/10.1186/1471-2105-7-153.
40. Kurcinski, M., Jamroz, M., Blaszczyk, M., Kolinski, A., and Kmiecik, S. (2015) CABS-dock web server for the flexible docking of peptides to proteins without prior knowledge of the binding site, *Nucleic Acids Res.*, **43**, 419-424, https://doi.org/10.1093/nar/gkv456.
41. Weng, G., Wang, E., Wang, Z., Liu, H., Zhu, F., Li, D., and Hou, T. (2019) HawkDock: a web server to predict and analyze the protein-protein complex based on computational docking and MM/GBSA, *Nucleic Acids Res.*, **47**, 322-330, https://doi.org/10.1093/nar/gkz397.
42. Gonzalez-Galarza, F. F., McCabe, A., Santos, E. J. M. D., Jones, J., Takeshita, L., Ortega-Rivera, N. D., Cid-Pavon, G. M. D., Ramsbottom, K., Ghattaoraya, G., Alfirevic, A., Middleton, D., and Jones, A. R. (2020) Allele frequency net database (AFND) 2020 update: gold-standard data classification, open access genotype data and new query tools, *Nucleic Acids Res.*, **48**, 783-788, https://doi.org/10.1093/nar/gkz1029.
43. Arai, R., Ueda, H., Kitayama, A., Kamiya, N., and Nagamune, T. (2001) Design of the linkers which effectively separate domains of a bifunctional fusion protein, *Protein Eng.*, **8**, 529-532, https://doi.org/10.1093/protein/14.8.529.
44. Meza, B., Ascencio, F., Sierra-Beltrán, A. P., Torres, J., and Angulo, C. (2017) A novel design of a multi-antigenic, multistage and multi-epitope vaccine against *Helicobacter pylori*: an *in silico* approach, *Infect. Genet. Evol.*, **49**, 309-317, https://doi.org/10.1016/j.meegid.2017.02.007.
45. Noderer, W. L., Flockhart, R. J., Bhaduri, A., Diaz de Arce, A. J., Zhang, J., Khavari, P. A., and Wang, C. L. (2014) Quantitative analysis of mammalian translation initiation sites by FACS-seq, *Mol. Syst. Biol.*, **10**, 748, https://doi.org/10.15252/msb.20145136.
46. Sample, P. J., Wang, B., Reid, D. W., Presnyak, V., McFadyen, I. J., Morris, D. R., and Seelig, G. (2019) Human 5′ UTR design and variant effect prediction from a massively parallel translation assay, *Nat. Biotechnol.*, **7**, 803-809, https://doi.org/10.1038/s41587-019-0164-5.
47. Reshetnikov, V., Terenin, I., Shepelkova, G., Yeremeev, V., Kolmykov, S., Nagornykh, M., Kolosova, E., Sokolova, T., Zaborova, O., Kukushkin, I., Kazakova, A., Kunyk, D., Kirshina, A., Vasileva, O., Seregina, K., Pateev, I., Kolpakov, F., and Ivanov, R. (2024) Untranslated region sequences and the efficacy of mRNA vaccines against tuberculosis, *Int. J. Mol. Sci.*, **25**, 888, https://doi.org/10.3390/ijms25020888.
48. Magnan, C. N., Zeller, M., Kayala, M. A., Vigil, A., Randall, A., Felgner, P. L., and Baldi, P. (2010) High-throughput prediction of protein antigenicity using protein microarray data, *Bioinformatics*, **23**, 2936-2943, https://doi.org/10.1093/bioinformatics/btq551.
49. Gasteiger, E., Gattiker, A., Hoogland, C., Ivanyi, I., Appel, R. D., and Bairoch, A. (2003) ExPASy: The proteomics server for in-depth protein knowledge and analysis, *Nucleic Acids Res.*, **13**, 3784-3788, https://doi.org/10.1093/nar/gkg563.
50. Yang, J., Anishchenko, I., Park, H., Peng, Z., Ovchinnikov, S., and Baker, D. (2020) Improved protein structure prediction using predicted interresidue orientations, *Proc. Natl. Acad. Sci. USA*, **3**, 1496-1503, https://doi.org/10.1073/pnas.1914677117.
51. Kringelum, J. V., Nielsen, M., Padkjær, S. B., and Lund, O. (2013) Structural analysis of B-cell epitopes in antibody:protein complexes, *Mol. Immunol.*, **53**, 24-34, https://doi.org/10.1016/j.molimm.2012.06.001.
52. Ponomarenko, J., Bui, H. H., Li, W., Fusseder, N., Bourne, P. E., Sette, A., and Peters, B. (2008) ElliPro: a new structure-based tool for the prediction of antibody epitopes, *BMC Bioinform.*, **9**, 514, https://doi.org/10.1186/1471-2105-9-514.
53. Solanki, V., and Tiwari, V. (2018) Subtractive proteomics to identify novel drug targets and reverse vaccinology for the development of chimeric vaccine against *Acinetobacter baumannii*, *Sci. Rep.*, **8**, 9044, https://doi.org/10.1038/s41598-018-26689-7.

54. Kozakov, D., Hall, D. R., Xia, B., Porter, K. A., Padhorny, D., Yueh, C., Beglov, D., and Vajda, S. (2017) The ClusPro web server for protein-protein docking, *Nat. Protoc.*, **2**, 255-278, https://doi.org/10.1038/nprot.2016.169.
55. Xue, L. C., Rodrigues, J. P., Kastritis, P. L., Bonvin, A. M., and Vangone, A. (2016) PRODIGY: a web server for predicting the binding affinity of protein-protein complexes, *Bioinformatics*, **23**, 3676-3678, https://doi.org/10.1093/bioinformatics/btw514.
56. Laskowski, R. A., Jabłońska, J., Pravda, L., Vařeková, R. S., and Thornton, J. M. (2018) PDBsum: Structural summaries of PDB entries, *Protein Sci.*, **1**, 129-134, https://doi.org/10.1002/pro.3289.
57. Rapin, N., Lund, O., Bernaschi, M., and Castiglione, F. (2010) Computational immunology meets bioinformatics: the use of prediction tools for molecular binding in the simulation of the immune system, *PLoS One*, **5**, e9862, https://doi.org/10.1371/journal.pone.0009862.
58. Zhang, H., Zhang, L., Lin, A., Xu, C., Li, Z., Liu, K., Liu, B., Ma, X., Zhao, F., Jiang, H., Chen, C., Shen, H., Li, H., Mathews, D. H., Zhang, Y., and Huang, L. (2023) Algorithm for optimized mRNA design improves stability and immunogenicity, *Nature*, **621**, 396-403, https://doi.org/10.1038/s41586-023-06127-z.
59. Diez, M., Medina-Muñoz, S. G., Castellano, L. A., da Silva Pescador, G., Wu, Q., and Bazzini, A. A. (2022) iCodon customizes gene expression based on the codon composition, *Sci. Rep.*, **12**, 12126, https://doi.org/10.1038/s41598-022-15526-7.
60. Meade, R. K., and Smith, C. M. (2024) Immunological roads diverged: mapping tuberculosis outcomes in mice, *Trends Microbiol.*, **33**, 15-33, https://doi.org/10.1016/j.tim.2024.06.007.
61. Eremeev, V. V., Dukhovlinov, I. V., Orlov, A. I., Shepelkova, G. S., Fedorova, E. A., Balazovsky, M. B., and Gergert, V. Ya. (2018) Study of the duration of the immune response induced by a vaccine based on recombinant proteins Ag85, TB10 and FliC [in Russian], *Med. Immunol.*, **20**, 271-276, https://doi.org/10.15789/1563-0625-2018-2-271-276.
62. Abou-Zeid, C., Gares, M. P., Inwald, J., Janssen, R., Zhang, Y., Young, D. B., Hetzel, C., Lamb, J. R., Baldwin, S. L., Orme, I. M., Yeremeev, V., Nikonenko, B. V., and Apt, A. S. (1997) Induction of a type 1 immune response to a recombinant antigen from *Mycobacterium tuberculosis* expressed in *Mycobacterium vaccae*, *Infect. Immun.*, **65**, 1856-1862, https://doi.org/10.1128/iai.65.5.1856-1862.1997.
63. Avdienko, V. G., Babayan, S. S., and Bocharova, I. V. (2024) Characteristics and application of monoclonal antibodies against *Mycobacterium kansasii* [in Russian], *Vestnik CNIIT*, **8**, 51-63, https://doi.org/10.57014/2587-6678-2024-8-4-51-63.
64. Kou, Y., Xu, Y., Zhao, Z., Liu, J., Wu, Y., You, Q., Wang, L., Gao, F., Cai, L., and Jiang, C. (2017) Tissue plasminogen activator (tPA) signal sequence enhances immunogenicity of MVA-based vaccine against tuberculosis, *Immunol. Lett.*, **190**, 51-57, https://doi.org/10.1016/j.imlet.2017.07.007.
65. Kreiter, S., Selmi, A., Diken, M., Sebastian, M., Osterloh, P., Schild, H., Huber, C., Türeci, O., and Sahin, U. (2008) Increased antigen presentation efficiency by coupling antigens to MHC class I trafficking signals, *J. Immunol.*, **1**, 309-318, https://doi.org/10.4049/jimmunol.180.1.309.
66. Yang, H., Chen, H., Liu, Z., Ma, H., Qin, L., Jin, R., Zheng, R., Feng, Y., Cui, Z., Wang, J., Liu, J., and Hu, Z. (2013) A novel B-cell epitope identified within *Mycobacterium tuberculosis* CFP10/ESAT-6 protein, *PLoS One*, **8**, e52848, https://doi.org/10.1371/journal.pone.0052848.
67. Ganguly, N., Siddiqui, I., and Sharma, P. (2008) Role of M. tuberculosis RD-1 region encoded secretory proteins in protective response and virulence, *Tuberculosis*, **88**, 510-517, https://doi.org/10.1016/j.tube.2008.05.002.
68. Yuan, Y., Crane, D. D., and Barry, C. E. (1996) Stationary phase-associated protein expression in *Mycobacterium tuberculosis*: function of the mycobacterial alpha-crystallin homolog, *J. Bacteriol.*, **178**, 4484-4492, https://doi.org/10.1128/jb.178.15.4484-4492.1996.
69. Cunningham, A. F., and Spreadbury, C. L. (1998) Mycobacterial stationary phase induced by low oxygen tension: cell wall thickening and localization of the 16-kilodalton alpha-crystallin homolog, *J. Bacteriol.*, **180**, 801-808, https://doi.org/10.1128/JB.180.4.801-808.1998.
70. Becker, K., and Sander, P. (2016) Mycobacterium tuberculosis lipoproteins in virulence and immunity – fighting with a double-edged sword, *FEBS Lett.*, **21**, 3800-3819, https://doi.org/10.1002/1873-3468.12273.
71. Ahmed, A., Das, A., and Mukhopadhyay, S. (2015) Immunoregulatory functions and expression patterns of PE/PPE family members: roles in pathogenicity and impact on anti-tuberculosis vaccine and drug design, *IUBMB Life*, **67**, 414-427, https://doi.org/10.1002/iub.1387.
72. Coler, R. N., Campos-Neto, A., Ovendale, P., Day, F. H., Fling, S. P., Zhu, L., Serbina, N., Flynn, J. L., Reed, S. G., and Alderson, M. R. (2001) Vaccination with the T cell antigen Mtb 8.4 protects against challenge with *Mycobacterium tuberculosis*, *J. Immunol.*, **166**, 6227-6235, https://doi.org/10.4049/jimmunol.166.10.6227.
73. Coppola, M., van den Eeden, S. J., Wilson, L., Franken, K. L., Ottenhoff, T. H., and Geluk, A. (2015) Synthetic long peptide derived from *Mycobacterium tuberculosis* latency antigen Rv1733c protects against tuberculosis, *Clin. Vaccine Immunol.*, **22**, 1060-1069, https://doi.org/10.1128/CVI.00271-15.
74. Fan, Q., Lu, M., Xia, Z. Y., and Bao, L. (2013) Mycobacterium tuberculosis MPT64 stimulates the activation

of murine macrophage modulated by IFN-γ, *Eur. Rev. Med. Pharmacol. Sci.*, **24**, 3296-3305.

75. Lin, M. Y., Geluk, A., Smith, S. G., Stewart, A. L., Friggen, A. H., Franken, K. L., Verduyn, M. J., van Meijgaarden, K. E., Voskuil, M. I., Dockrell, H. M., Huygen, K., Ottenhoff, T. H., and Klein, M. R. (2007) Lack of immune responses to Mycobacterium tuberculosis DosR regulon proteins following *Mycobacterium bovis* BCG vaccination, *Infect. Immun.*, **75**, 3523-3530, https://doi.org/10.1128/IAI.01999-06.
76. Sharpe, M. L., Gao, C., Kendall, S. L., Baker, E. N., and Lott, J. S. (2008) The structure and unusual protein chemistry of hypoxic response protein 1, a latency antigen and highly expressed member of the DosR regulon in Mycobacterium tuberculosis, *J. Mol. Biol.*, **383**, 822-836, https://doi.org/10.1016/j.jmb.2008.07.001.
77. Yao, L., Hu, Q., Chen, S., Zhou, T., Yu, X., Ma, H., Ghonaim, A., Wu, H., Sun, Q., Fan, S., and He, Q. (2021) Recombinant pseudorabies virus with TK/gE Gene deletion and Flt3L co-expression enhances the innate and adaptive immune response via activating dendritic cells, *Viruses*, **13**, 691, https://doi.org/10.3390/v13040691.
78. Boopathy, A. V., Nekkalapudi, A., Sung, J., Schulha, S., Jin, D., Sharma, B., Ng, S., Lu, S., Wimmer, R., Suthram, S., Ahmadi-Erber, S., Lauterbach, H., Orlinger, K. K., Hung, M., Carr, B., Callebaut, C., Geleziunas, R., Kuhne, M., Schmidt, S., and Falkard, B. (2024) Flt3 agonist enhances immunogenicity of arenavirus vector-based simian immunodeficiency virus vaccine in macaques, *J. Virol.*, **7**, e0029424, https://doi.org/10.1128/jvi.00294-24.
79. Zhu, J., Ke, Y., Liu, Q., Yang, J., Liu, F., Xu, R., Zhou, H., Chen, A., Xiao, J., Meng, F., Yu, L., Li, R., Wei, J., and Liu, B. (2022) Engineered Lactococcus lactis secreting Flt3L and OX40 ligand for *in situ* vaccination-based cancer immunotherapy, *Nat. Commun.*, **13**, 7466, https://doi.org/10.1038/s41467-022-35130-7.
80. Maraskovsky, E., Brasel, K., Teepe, M., Roux, E. R., Lyman, S. D., Shortman, K., and McKenna, H. J. (1996) Dramatic increase in the numbers of functionally mature dendritic cells in Flt3 ligand-treated mice: multiple dendritic cell subpopulations identified, *J. Exp. Med.*, **184**, 1953-1962, https://doi.org/10.1084/jem.184.5.1953.
81. Brasel, K., De Smedt, T., Smith, J. L., and Maliszewski, C. R. (2000) Generation of murine dendritic cells from flt3-ligand-supplemented bone marrow cultures, *Blood*, **96**, 3029-3039, https://doi.org/10.1182/blood.V96.9.3029.h8003029_3029_3039.
82. Pulendran, B., Banchereau, J., Burkeholder, S., Kraus, E., Guinet, E., Chalouni, C., Caron, D., Maliszewski, C., Davoust, J., Fay, J., and Palucka, K. (2000) Flt3-ligand and granulocyte colony-stimulating factor mobilize distinct human dendritic cell subsets *in vivo*, *J. Immunol.*, **165**, 566-572, https://doi.org/10.4049/jimmunol.165.1.566.
83. Triccas, J. A., Shklovskaya, E., Spratt, J., Ryan, A. A., Palendira, U., Fazekas de StGroth, B., and Britton, W. J. (2007) Effects of DNA- and *Mycobacterium bovis* BCG-based delivery of the Flt3 ligand on protective immunity to Mycobacterium tuberculosis, *Infect. Immun.*, **75**, 5368-5375, https://doi.org/10.1128/IAI.00322-07.
84. Ahn, S. S., Jeon, B. Y., Kim, K. S., Kwack, J. Y., Lee, E. G., Park, K. S., Sung, Y. C., and Cho, S. N. (2012) Mtb32 is a promising tuberculosis antigen for DNA vaccination in pre- and post-exposure mouse models, *Gene Ther.*, **19**, 570-575, https://doi.org/10.1038/gt.2011.140.
85. Xu, J., Xu, W., Chen, X., Zhao, D., and Wang, Y. (2008) Recombinant DNA vaccine of the early secreted antigen ESAT-6 by *Mycobacterium tuberculosis* and Flt3 ligand enhanced the cell-mediated immunity in mice, *Vaccine*, **26**, 4519-4525, https://doi.org/10.1016/j.vaccine.2008.06.044.
86. Branger, J., Leemans, J. C., Florquin, S., Weijer, S., Speelman, P., and Van Der Poll, T. (2004) Toll-like receptor 4 plays a protective role in pulmonary tuberculosis in mice, *Int. Immunol.*, **3**, 509-516, https://doi.org/10.1093/intimm/dxh052.
87. Xin, Q., Niu, H., Li, Z., Zhang, G., Hu, L., Wang, B., Li, J., Yu, H., Liu, W., Wang, Y., Da, Z., Li, R., Xian, Q., Wang, Y., Zhang, Y., Jing, T., Ma, X., and Zhu, B. (2013) Subunit vaccine consisting of multi-stage antigens has high protective efficacy against *Mycobacterium tuberculosis* infection in mice, *PLoS One*, **8**, e72745, https://doi.org/10.1371/journal.pone.0072745.
88. Oksanen, K. E., Myllymäki, H., Ahava, M. J., Mäkinen, L., Parikka, M., and Rämet, M. (2016) DNA vaccination boosts Bacillus Calmette-Guérin protection against mycobacterial infection in zebrafish, *Dev. Comp. Immunol.*, **54**, 89-96, https://doi.org/10.1016/j.dci.2015.09.001.
89. Vakili, B., Nezafat, N., Zare, B., Erfani, N., Akbari, M., Ghasemi, Y., Rahbar, M. R., and Hatam, G. R. (2020) A new multi-epitope peptide vaccine induces immune responses and protection against Leishmania infantum in BALB/c mice, *Med. Microbiol. Immunol.*, **209**, 69-79, https://doi.org/10.1007/s00430-019-00640-7.
90. Kozlova, A., Pateev, I., Shepelkova, G., Vasileva, O., Zakharova, N., Yeremeev, V., Ivanov, R., and Reshetnikov, V. (2024) A cap-optimized mRNA encoding multiepitope antigen ESAT6 induces robust cellular and humoral immune responses against *Mycobacterium tuberculosis*, *Vaccines (Basel)*, **12**, 1267, https://doi.org/10.3390/vaccines12111267.
91. Shepelkova, G. S., Reshetnikov, V. V., Avdienko, V. G., Sheverev, D. V., Yeremeev, V. V., and Ivanov, R. A. (2023) Impact of untranslated mRNA sequences on immunogenicity of mRNA vaccines against *M. tuberculosis* in mice, *Bull. RSMU*, **6**, 27-33, https://doi.org/10.24075/brsmu.2023.054.

92. Wu, M., Li, M., Yue, Y., and Xu, W. (2016) DNA vaccine with discontinuous T-cell epitope insertions into HSP65 scaffold as a potential means to improve immunogenicity of multi-epitope *Mycobacterium tuberculosis* vaccine, *Microbiol. Immunol.*, **60**, 634-645, https://doi.org/10.1111/1348-0421.12410.
93. Cai, H., Tian, X., Hu, X., Pan, Y., Li, G., Zhuang, Y., and Zhu, Y. (2003) Immunogenicity and protective efficacy study using combination of four tuberculosis DNA vaccines, *Sci. China C. Life Sci.*, **46**, 495-502, https://doi.org/10.1360/02yc0121.